Available online at www.sciencedirect.com
SCIENCE DIRECT
Thermochimica Acta 432 (2005) 47–55
thermochimica acta
www.elsevier.com/locate/tca

Effect of reaction temperature on the chlorination of a Sm_2O_3–CeO_2–C mixture

M.R. Esquivel [a,*], A.E. Bohé [b], D.M. Pasquevich [a,b]

[a] *Comisión Nacional de Energía Atómica, Centro Atómico Bariloche, RG8402AGP S.C. de Bariloche, Río Negro, Argentina*
[b] *Consejo Nacional de Investigaciones Científicas y Técnicas, Centro Atómico Bariloche, RG8402AGP S.C. de Bariloche, Río Negro, Argentina*

Received 5 November 2004; received in revised form 17 March 2005; accepted 11 April 2005

Abstract

The chlorination of a Sm_2O_3–CeO_2–C mixture with gaseous chlorine was studied by thermogravimetry (TG). The effect of the reaction temperature between 400 and 950 °C on the reaction rate was analyzed. The reaction products were studied by X-ray diffraction (XRD) and energy dispersive spectroscopy (EDS). Compared to the results previously found in the individual systems, it was concluded that each oxide evolves as being an individual in the mixture. Combined with TG results along with observations done using scanning electron microscopy (SEM), the stoichiometries of the reactions involved were obtained. From these results, a two-stage separation method for both oxides was proposed.

Keywords: Chlorination; Gas–solid; Samarium sesquioxide; Cerium dioxide

1. Introduction

The importance of both cerium and samarium compounds has increased markedly in the last decades. As pure oxides, both lanthanides are used in fuel cells [1,2]. Cerium oxide is used in catalysis [3,4] while samarium as either oxychloride, oxide or metal is used in permanent magnets and for unique optical materials [5,6]. The marked chemical similarities [7] between lanthanide oxides along with their high stability [8] make separation a difficult task. To overcome this problem, different separation methods have been proposed [9–11].

The chlorination and carbochlorination of Sm_2O_3 and CeO_2 and their mixture were previously studied [12–16]. Reaction products were identified and by TG analysis, the stoichiometry of these reactions was obtained [12–16].

CeO_2 carbochlorination starts above 700 °C producing $CeCl_3$ (s, l, g) [13] and Sm_2O_3 carbochlorination starts over 400 °C [12] producing SmOCl (s) in one stage up to 650 °C and SmOCl (s) and $SmCl_3$ (s, l, g) in two successive stages from 650 to 950 °C [12].

These differences in reactivity towards C (s) + Cl_2 (g) [12,13] suggest using this difference to separate these oxides. The chlorides and oxychlorides formed occur in different agregation states and have differences in their vapor pressures suggests separation by physical methods such as volatilization or fractional distillation.

2. Experimental

2.1. Materials and procedure

Ar 99.999% purity (AGA, Argentina), Cl_2 99.8% (Indupa, Argentina) and raw Sm_2O_3, CeO_2 and C were the reactants used. These solids were previously characterized [12–16]. These reactants were weighed and mixed mechanically to obtain a CeO_2 (45 wt%)–Sm_2O_3 (45 wt%)–C (10 wt%) mixture. The percentage of each oxide was determined using the Rietveld method [17] (see appendix for sample

* Corresponding author. Tel.: +54 2944 445293/5337; fax: +54 2944 445299.
E-mail address: esquivel@cab.cnea.gov.ar (M.R. Esquivel).

0040-6031/$ – see front matter © 2005 Elsevier B.V. All rights reserved.
doi:10.1016/j.tca.2005.04.011

Nomenclature

a	cell parameter (Å)
b	cell parameter (Å)
c	cell parameter (Å)
D	diffusion coefficient ($m^2\,s^{-1}$)
E_{ap}	apparent activation energy ($kJ\,mol^{-1}$)
f	stoichiometric correction coefficient (dimensionless)
FW	formula weight ($kg\,mol^{-1}$)
g	coefficient that relates Δw to the mass change of carbon, CeO_2 and Sm_2O_3 (dimensionless)
L	characteristic dimension of the sample (m)
m_0	initial mass sample (mg)
Δm	mass variation (mg)
ΔM	balance mass variation (mg)
N	molar flow of chlorine ($mol\,s^{-1}$)
NTP	normal pressure and temperature conditions
r	reaction rate (s^{-1})
R	reaction rate ($mol\,s^{-1}$)
t	time (s)
T	temperature (°C)
z	adjustable parameter

Greek symbols

α	cell angle (°)
α_{C,Sm_2O_3}	carbon, Sm_2O_3 reaction degree (dimensionless)
β	cell angle (°)
γ	cell angle (°)
ν	kinematic viscosity ($m^2\,s^{-1}$)

parameters detail). Carbon percentage was determined by weighing it before and after burning the mixture at 950 °C [12,13,16].

A thermogravimetric analyzer based on a Cahn 2000 electrobalance described elsewhere [18] was used to measure the chlorination rate. The mass change resolution of the system was ±10 μg under the experimental conditions [12,13,15]. Samples of Sm_2O_3–CeO_2–C of 10 mg were placed inside a quartz crucible suspended by a quartz fiber inside a furnace. Isothermal and non-isothermal measurements were made under an overall pressure of 101.3 kPa and a total gas flow rate of $7.9\,l\,h^{-1}$ (NPT). In the isothermal experiments, samples were first heated for 1 h in Ar at the desired operation temperature, then Cl_2 was injected into the system reaching a $pCl_2 = 30.3$ kPa.

In the temperature scanning experiments, samples were heated from room temperature to 950 °C at 2.6 °C min^{-1} at a $pCl_2 = 30.3$ kPa in flowing Ar–Cl_2. In both cases, mass changes were measured and apparent mass changes were corrected as explained elsewhere [18]. Since the reaction products, $SmCl_3$ and $CeCl_3$, are hygroscopic [19], samples were treated and auxiliary measurements done in a globe box [12–15].

2.2. Expression of results

For non-isothermal runs, TG data are expressed as Δw versus T, where Δw and T are the mass change in milligrams and the temperature in °C, respectively. For isothermal runs, TG data are expressed as either the fractional carbon mass loss given by $\alpha_C = \Delta m(C)/m_0(C)$, where $\Delta m(C)$ and $m_0(C)$ are the carbon mass change and carbon initial mass, respectively, or the fractional samarium oxide mass loss given by $\alpha_{Sm_2O_3} = \Delta m(Sm_2O_3)/m_0(Sm_2O_3)$. Either Sm_2O_3 or carbon consumption is related to the observed mass change by $\Delta m(C \text{ or } Sm_2O_3) = g\,\Delta w$. g is a coefficient which relates the Δw to the mass change of carbon, CeO_2 and Sm_2O_3, and which depends on both the stoichiometry of the reaction and the aggregation state of reactants and products. Then, the reaction degree is transformed to:

$$\alpha_{C,Sm_2O_3} = \frac{g\,\Delta m(C, Sm_2O_3)}{m_{0(C,Sm_2O_3)}} \quad (1)$$

where the parenthesis indicates that the symbol contained within the formula corresponds to either carbon or Sm_2O_3.The reaction rate (s^{-1}) is:

$$r = -\frac{d\alpha_{C,Sm_2O_3}}{dt} = -\frac{g}{m_{0(C,Sm_2O_3)}}\frac{dm}{dt} \quad (2)$$

The reaction rate ($mol\,Cl_2\,s^{-1}$) is:

$$R = \frac{dn_{Cl_2}}{dt} = \frac{f m_{0(C,Sm_2O_3)} \cdot r}{FW(C, Sm_2O_3)} \quad (3)$$

where n is the moles of chlorine, f a coefficient that relates the stoichiometric consumption of moles of either carbon or Sm_2O_3 to moles of chlorine and FW is the formula weight of either carbon or Sm_2O_3.

3. Results and discussion

3.1. Reactivity of the CeO_2–Sm_2O_3–C system with chlorine and reaction products

Non-isothermal experiments were made to determine the main products of reaction from room temperature to 950 °C. The corrected TG curve is shown in curve (1) in Fig. 1. For comparison, the corrected TG curves of the individual carbochlorination of both CeO_2 (2) [13] and Sm_2O_3 (3) [12] are also shown. In the CeO_2–Sm_2O_3–Cl_2–C system, the starting temperature of reaction (190 °C) is indicated by "A" in the curve. As temperature raises, the mass increases reaching a maximum at 350 °C where a flat zone corresponding to the formation of a condensed phase is indicated by "B". Slow formation of another condensed phase is observed up to 480 °C ("C"), followed by a flat zone. Above 650 °C, a further slow mass gain extends up to 700 °C ("D"). Between 700

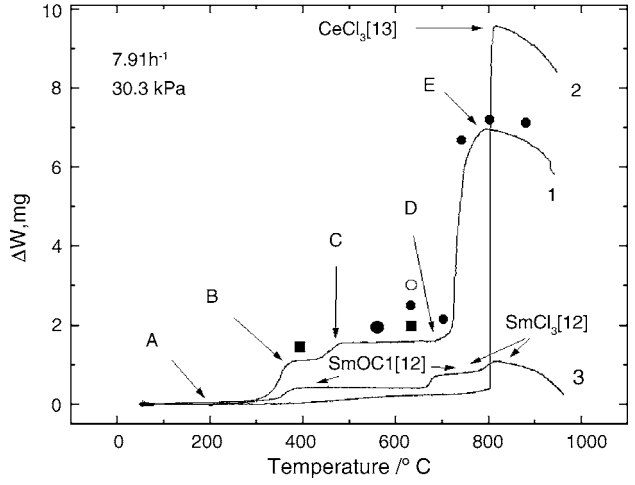

Fig. 1. (1) Non-isothermal curve of the chlorination of Sm_2O_3–CeO_2–C. XRD, EDS and SEM observations are indicated by full circles, hollow circles and full squares, respectively. (2) Non-isothermal curve of the chlorination of CeO_2–C [13]. (3) Non-isothermal curve of the chlorination of Sm_2O_3–C [12]. Reaction products [12,13] are labeled in the figure.

and 800 °C ("E"), a marked mass gain occurs. Above 800 °C, an increasing rate of mass loss is observed up to 950 °C. This mass loss is attributed to vaporization of the reaction products. This curve resembles the curves for the individual carbochlorination of Sm_2O_3 [12] and CeO_2 [13] suggesting formation of similar products. Differences in mass gain between the mixture and the individual oxide in each temperature range are attributed to the differences in the C content in the initial mixtures [12,13]. The identity of phases formed in each of the individual systems [12,13] are labeled in Fig. 1.

To identify the reaction products, isothermal experiments were done at selected temperatures and the reaction products were characterized by XRD, EDS and SEM at the points on the TG curve of Fig. 1 indicated by full circles, hollow circles and full squares, respectively. With the aid of mass balances, the stoichiometries of the reactions involved were assessed.

3.2. Stoichiometries and reaction products between 400 and 625 °C

Four hundred and 550 °C were selected as representative temperatures in this range. The diffraction patterns of the reaction products at 3 min (a), 20 min (b) and 40 min (c) at 550 °C along with the reference patterns of CeO_2 [20] (d) Sm_2O_3 [21] (e) and SmOCl [22] (f) are displayed in Fig. 2. SmOCl diffraction lines increase with time as the ones of Sm_2O_3 decreases. No Ce compound other than CeO_2 is observed. No product of interaction between Sm and Ce is observed in the diffraction patterns. SEM images of reaction products at 400 °C show chemical attack in the shape of pits on the carbon indicating it is involved in the reaction [12,13]. These results along with mass balances at various temperatures lead to the conclusion that in this temperature range

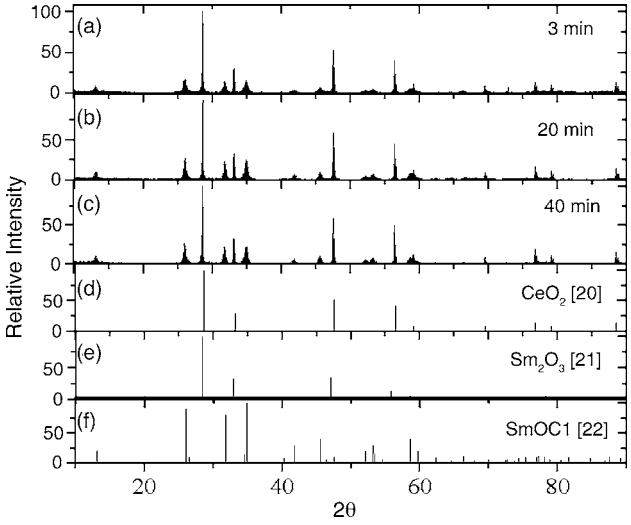

Fig. 2. Diffraction patterns of the reaction products at 550 °C.

only Sm_2O_3 reacts with the stoichiometry,

$$2Sm_2O_3\,(s) + 2Cl_2\,(g) + C\,(s) = 4SmOCl\,(s) + CO_2\,(g) \quad (4)$$

XRD and SEM analysis performed at temperatures lower than 400 °C indicated that only direct chlorination of Sm_2O_3 occurs [12,14]. Like the individual CeO_2–Cl_2 system [15], no chlorination of the CeO_2 present in the Sm_2O_3–CeO_2–C mixture is observed.

3.3. Stoichiometries and reaction products between 650 and 700 °C

Six hundred and fifty and 700 °C were selected for analysis of the reaction products. The diffraction patterns obtained at various times at both temperatures are shown in Fig. 3. At

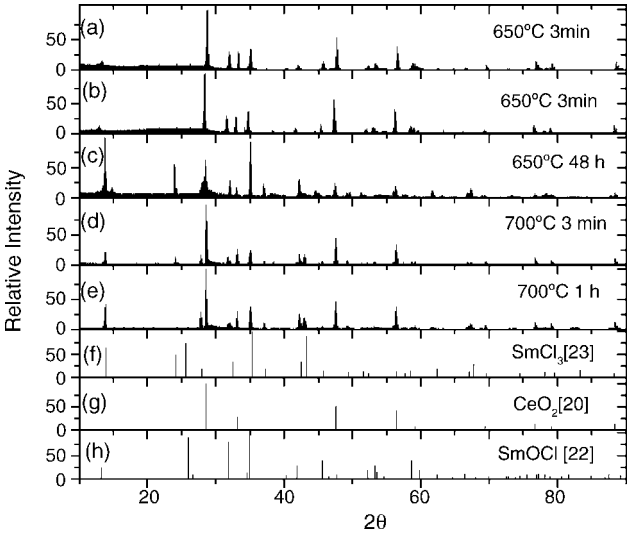

Fig. 3. Diffraction patterns of the reaction products at 650 and 700 °C.

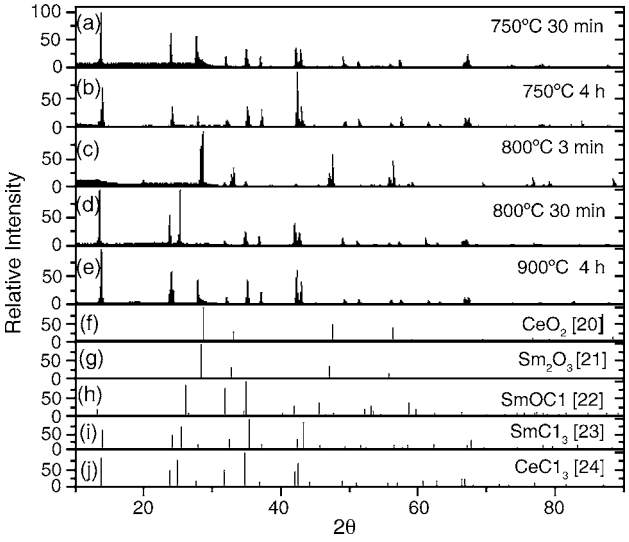

Fig. 4. Diffraction patterns of the reaction products at 750, 800 and 900 °C [20–24].

shorter times at both temperatures (Fig. 3a and d), the formation of SmOCl is detected. At longer times, the further carbochlorination of this oxychloride leads to the formation of $SmCl_3$. This product is incompletely obtained at 650 °C (Fig. 3c). At 700 °C, the successive formation of both compounds is observed but no SmOCl is detected at longer times (Fig. 3e). No products of the carbochlorination of CeO_2 are observed in this temperature range (Fig. 3a–e). These results are in agreement with those obtained from the individual carbochlorination of each oxide [12,13]. A SEM image of the reaction products at 650 °C analyzed by EDS shows $SmCl_3$ particles that were vaporized during the preparation of the sample. These results along with mass balances led to the conclusion that only Sm_2O_3 reacts in two steps, the first one defined by Eq. (4) and the second one,

$$2Sm_2O_3\,(s) + 3C\,(s) + 6Cl_2\,(g) = 4SmCl_3 + 3CO_2\,(g) \quad (5)$$

which is the same as the individual carbochlorination of Sm_2O_3 [12].

3.4. Stoichiometries and reaction products between 700 and 950 °C

Seven hundred and fifty, 800 and 900 °C were selected as the representative temperatures in this range. The reaction products obtained at these temperatures at various times along with the reference patterns are shown in Fig. 4. At shorter times at 750 and 800 °C, formation of SmOCl is observed. At longer times, both $SmCl_3$ and $CeCl_3$ are detected. These results are the same as the individual carbochlorination of each oxide [12,13]. As observed at the lower temperatures (Figs. 2 and 3), no interaction between cerium and samarium compounds is observed. Mass balances in this temperature range indicate that CeO_2 is carbochlorinated according to

$$2CeO_2\,(s) + 3Cl_2\,(g) + 4C\,(s) = 2CeCl_3\,(l,\ s) + 4CO\,(g) \quad (6)$$

which is the same stoichiometry as that of the individual carbochlorination [13]. Like the Sm_2O_3–Cl_2–C system [12], the mass balances indicated that Sm_2O_3 is carbochlorinated in two steps. Between 700 and 850 °C, SmOCl is produced according to Eq. (4). At higher temperatures, the formation of SmOCl as a first step is observed but no stoichiometry can be assigned. At 725 °C, the second step leads to the carbochlorination of SmOCl to produce $SmCl_3$ according to

$$2SmOCl\,(s) + 2Cl_2\,(g) + C\,(s) = 2SmCl_3\,(l,\ s) + CO_2\,(g) \quad (7)$$

And between 750 and 950 °C:

$$SmOCl\,(s) + Cl_2\,(g) + C\,(s) = SmCl_3\,(l,\ s) + CO\,(g) \quad (8)$$

The global reaction at 725 °C is described by:

$$3Sm_2O_3\,(s) + 6Cl_2\,(g) + 3C\,(s) = 4SmCl_3\,(l,\ s) + 3CO_2\,(g) \quad (9)$$

While the global reaction between 750 and 950 °C is described by:

$$3Sm_2O_3\,(s) + 6Cl_2\,(g) + 6C\,(s) = 4SmCl_3\,(l,\ s) + 6CO\,(g) \quad (10)$$

Traces of both $CeCl_3$ and $SmCl_3$ were observed on SEM images which is in agreement with their respective melting points of 816 and 681 °C [25].

3.5. Effect of the temperature on the reaction rate

Isothermal TG curves are shown in Fig. 5. At $T \leq 675$ °C, the carbochlorination is achieved in one step corresponding to the formation of SmOCl according to Eq. (4). The rate increases as the temperature is raised, i.e., time needed to achieve $\alpha_{Sm_2O_3} = 0.9$ is 607, 90 and 20 s at 400, 500 and 600 °C, respectively. Table 1 displays reaction rates calculated at various $\alpha_{Sm_2O_3}$ by Eq. (3) along with the theoretical values obtained from the equation of Ranz-Marshall [12–15] corrected as suggested [26]. Since both sets of values are similar, it is concluded that carbochlorination of the mixture is achieved under external mass transfer control which increases as temperature increases [12,15]. The values are also compared to those for the individual carbochlorination systems [12,13]. The values in the mixture are of the same order of magnitude as those for carbochlorination of Sm_2O_3 [12] indicating that no changes are produced due to the presence of CeO_2 in the mixture. CeO_2 presents no reaction in this temperature range which is also in agreement with the individual system [13].

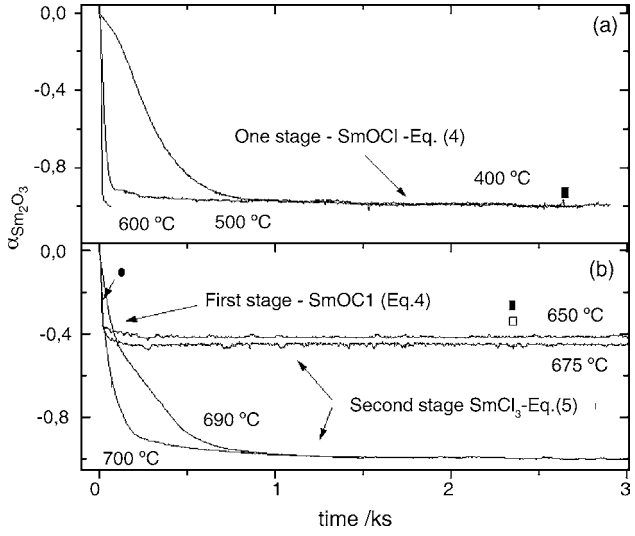

Fig. 5. (a) Effect of the temperature between 400 and 625 °C. The global stoichiometry is calculated using Eq. (4). (b) Effect of the temperature between 650 and 700 °C. In these curves, the global stoichiometry is calculated according to Eq. (5). Formation of products at each stage from XRD, EDS and SEM measurements are signaled by full circles, hollow circles and full squares, respectively.

The TG curves corresponding to 650–700 °C are displayed in Fig. 5b. At 650 and 675 °C, carbochlorination of Sm_2O_3 leads to a complete formation of SmOCl in the first stage but not to the full formation of $SmCl_3$ in the second. At temperatures higher than 675 °C, formation of $SmCl_3$ is complete according to Eq. (5). This behavior was previously observed in the carbochlorination of Sm_2O_3 [12]. The experimental reaction rates are compared to those of the Ranz-Marshall equation [12–15] in Table 1. The first stage reaction rate is similar to those of the Ranz-Marshall equation indicating the first stage is controlled by mass transfer. The second stage is two orders of magnitudes lower suggesting a different reaction regime closer to chemical-mixed control. Similar experimental reaction rates values and the presence of two reaction stages in this temperature range were observed in the individual carbochlorination of Sm_2O_3 [12] suggesting no interaction with CeO_2 in the mixture. As discussed in Section 3.3, the carbochlorination of CeO_2 is not achieved in this temperature range.

The TG curves at 725–950 °C are displayed in Fig. 6. In this case, curves are expressed as the consumption of carbon because this reactant is the one common to reaction of both oxides. Like that of Sm_2O_3 [12], the carbochlorination of the mixture occurs in two stages. In the first, formation of SmOCl is achieved. (Fig. 4a and c). In the second, the formation of both $SmCl_3$ and $CeCl_3$ is achieved (Fig. 4b, d and e). As also observed in the carbochlorination of Sm_2O_3 [12], the rate in the second stage is more dependent on temperature than the first. The time to reach $\alpha_C = 0.20$ is 10, 17 and 20 s at 950, 800 and 725 °C, while the time to reach $\alpha_C = 0.80$ is 50, 168 and 461 s at the same temperatures, respectively.

Table 1 displays the carbochlorination rate at various temperatures and α_C using Eq. (3) with the global stoichiometry of Eqs. (6), (9) and (10). The carbochlorination rates at lower α_C values are faster, by at least one order of magnitude, than those at higher α_C values at the same temperatures. This indicates the reaction evolves under different kinetic regimes. As discussed in the previous section, the first stage is un-

Table 1
Comparison between r (experimental) and N (theoretical) reaction rates

T (°C)	D (cm s^{-2})	ν (cm s^{-2})	N (mol Cl_2 s^{-2})	Equation used	α	R (mol Cl_2 s^{-2})		
						This work	[12]	[13]
400	0.43	0.39	6.01×10^{-8}	(4)	0.2	3.28×10^{-8}	1.15×10^{-8}	–
					0.5	2.71×10^{-8}	1.27×10^{-8}	–
600	0.76	0.67	4.30×10^{-7}	(4)	0.2	9.64×10^{-8}	4.42×10^{-7}	–
					0.5	4.78×10^{-8}	5.98×10^{-7}	–
650	0.83	0.74	4.57×10^{-7}	(4)	0.2	9.75×10^{-7}	3.76×10^{-7}	–
				(5)	0.45	7.00×10^{-10}	7.37×10^{-10}	–
700	0.92	0.81	5.00×10^{-7}	(5)	0.2	8.16×10^{-7}	8.05×10^{-7}	–
					0.5	1.25×10^{-9}	1.67×10^{-9}	–
750	1.00	0.89	5.28×10^{-7}	(6), (10)	0.2	8.45×10^{-7}	5.25×10^{-7}	–
					0.5	7.10×10^{-9}	2.0×10^{-9}	–
800	1.09	0.96	6.00×10^{-7}	(6), (10)	0.2	8.62×10^{-7}	3.02×10^{-7}	3.67×10^{-7}
					0.5	9.02×10^{-9}	6.02×10^{-9}	1.50×10^{-7}
850	1.18	1.04	7.52×10^{-7}	(6), (10)	0.2	8.76×10^{-7}	5.86×10^{-7}	4.70×10^{-7}
					0.5	5.00×10^{-8}	8.04×10^{-9}	3.27×10^{-7}
950	1.36	1.21	8.01×10^{-7}	(6), (10)	0.2	9.90×10^{-7}	7.32×10^{-7}	6.91×10^{-7}
					0.5	5.78×10^{-8}	1.78×10^{-8}	2.40×10^{-7}

Values of D and ν at various temperatures are estimated for $pCl_2 = 30.3$ kPa. N values are calculated according to the Ranz-Marshall equation and corrected as suggested [15,26]. In this equation, $L = 0.30$. The experimental values of R are obtained for 10 mg of Sm_2O_3–CeO_2–C under a $pCl_2 = 30.3$ kPa and a total gas flow rate of 7.91 l h^{-1} at each temperature. Eighth and ninth columns display these values for the individual carbochlorination of Sm_2O_3 [12] and CeO_2 [13].

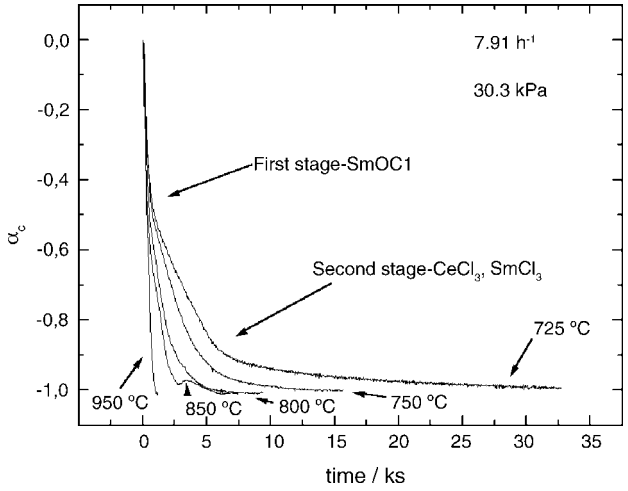

Fig. 6. Effect of the temperature between 725 and 950 °C. In this case, $g = 0.5399$. Sm_2O_3 global consumption is expressed according to Eqs. (9) and (10) at 725 and 750 to 950 °C, respectively. CeO_2 global consumption is calculated according to Eq. (6).

der external mass transfer. Unlike the 625–700 °C temperature range in which the first and second stages differ by at least two orders of magnitude, both stages in this temperature range differs by only one order of magnitude, as observed in Table 1. This indicates that external mass transfer controls the first stage and influences, not controls, the second stage in this temperature range [27]. This behavior was observed previously in the Sm_2O_3–C–Cl_2 system [12].

3.6. The activation energy and regimes of reaction

3.6.1. The formation of SmOCl

The calculation of the activation energy for the formation of SmOCl in the 400–850 °C range is shown in Fig. 7. Between 400 and 625 °C, the E_{ap} value is $79 \pm 3\,kJ\,mol^{-1}$. At 625 °C, the lines break. The E_{ap} value calculated between 625 and 850 °C is $12 \pm 3\,kJ\,mol^{-1}$, only some reaction degrees are shown, but calculation was done for values between 0.1 and 0.9. The E_{ap} values are lower and the temperature were the lines break is higher than those of the carbochlorination of Sm_2O_3 [12] (see Table 2). This effect is attributed to the presence of a higher amount of C available to react with the Sm_2O_3 present in the mixture.

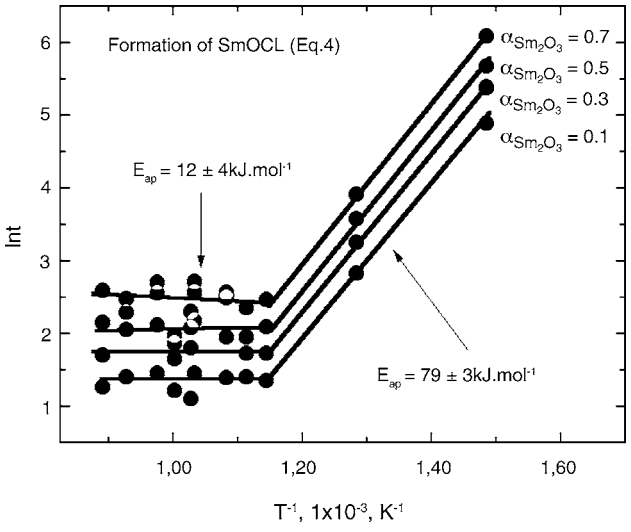

Fig. 7. Plot of $\ln t$ vs. T^{-1} at various conversions for 10 mg of CeO_2–Sm_2O_3–C between 400 and 850 °C. The stoichiometry considered corresponds to Eq. (4).

Table 2
Activation energy for the formation of SmOCl and $SmCl_3$–$CeCl_3$ in the carbochlorination of the CeO_2–Sm_2O_3 mixture

Process	Temperature range (°C)	α Range	E_{ap} ($kJ\,mol^{-1}$)
SmOCl formation	400–625	0.10–0.90	79 ± 3
	650–850	0.10–0.90	12 ± 4
$SmCl_3$–$CeCl_3$ formation	725–950	0.10–0.50	12 ± 4
		0.60–0.90	75 ± 3

3.6.2. The formation of $CeCl_3$ and $SmCl_3$

Like that of the carbochlorination of Sm_2O_3 [12], the formation of $SmCl_3$ occurs as a second stage after the formation of SmOCl. No total conversion of the SmOCl is achieved at temperatures lower than 690 °C as observed in both Figs. 5b and 3a–c. The formation of solid $SmCl_3$ hindering the progress of the reaction is attributed to this discontinuity of the reaction curves at temperatures lower than 690 °C as observed in Fig. 5b.

If compared with the curves of the carbochlorination of Sm_2O_3 [12], those of the carbochlorination of the CeO_2–Sm_2O_3 mixture shown in Fig. 5 are quicker. As example, the time to reach $\alpha_{Sm_2O_3} = 0.4$ and 0.8 at 700 °C are 27 and 141 s for the CeO_2–Sm_2O_3 mixture, while it is 119 and 3046 s for the individual carbochlorination of Sm_2O_3 [12]. This effect is attributed to the presence of a higher amount of carbon available to react with the Sm_2O_3 in the mixture than that available in the individual carbochlorination [12]. Despite the fact that the percentage of carbon in the Sm_2O_3–C [12] and that in Sm_2O_3–CeO_2–C are approximately the same, the total amount of C in the samples of the mixture are higher because these samples have a total mass four times higher. As studied in a previous work [13], carbon produces a kinetic effect which accelerates the ratio of reaction [13]. It is attributed to the presence of intermediaries of reaction incremented with the amount of carbon present in the sample and available to react [13]. At temperatures higher than 700 °C, this increment on the reaction ratio is also due to the formation of liquid $SmCl_3$. As discussed in a previous work [12], the formation of $SmCl_3$ (l) enhances the diffusion of reactive species from or to the reactive SmOCl surface and favoring the carbochlorination of Sm_2O_3 in the process. This process also favors the carbochlorination of CeO_2. As observed in Fig. 6, the carbochlorination of CeO_2 according to Eq. (6) and that of Sm_2O_3 according to Eqs. (9) and (10) in the mix-

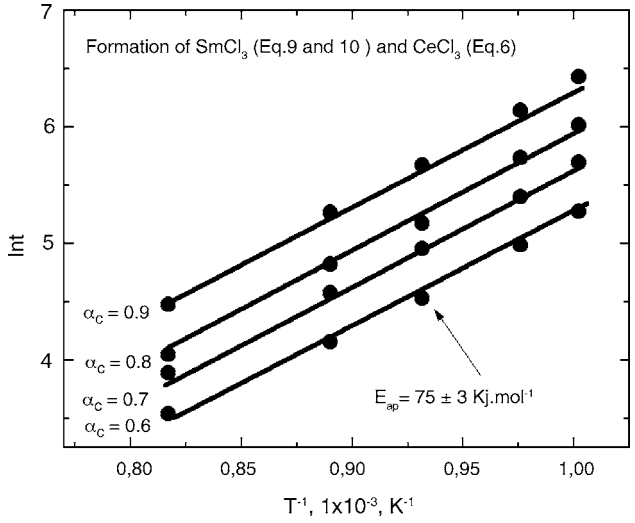

Fig. 8. Plot of $\ln t$ vs. T^{-1} at various conversions for 10 mg of CeO_2–Sm_2O_3–C between 700 and 950 °C. The stoichiometries considered correspond to Eqs. (6), (9) and (10).

ture are completed. Although the individual carbochlorination of Sm_2O_3 is completed in this temperature range [12], that of CeO_2 is not [13]. This last reaction only achieves the maximum α_{CeO_2} at temperatures higher than 790 °C [13]. In CeO_2 carbochlorination, the formation of liquid $CeCl_3$ enhances the completion of the reaction at higher temperatures by coalescing and leaving unreacted CeO_2 surface exposed to chlorine chemical attack [13]. When CeO_2–Sm_2O_3–C is chlorinated, the formation of liquid $SmCl_3$ at lower temperatures due to its mp of 681 °C [25] not only coalesces and exposes the SmOCl surface to further carbochlorination as observed in Fig. 6, but also exposes the CeO_2 surface to react and the full carbochlorination of both oxides is favored in the process. At temperatures higher than 800 °C, the presence of carbon which accelerates the carbochlorination rate of the mixture and the simultaneous formation of $SmCl_3$ (l) and $CeCl_3$ (l) (mp 816 °C [25]) produces a global increment of the reaction rate. This combined effect is observed in the E_{ap} values of the reaction. The E_{ap} values calculated in this temperature range are shown in Fig. 8. Although only four α values are shown, the calculation was done for α between 0.1 and 0.9. The calculation of α between 0.1 and 0.5 (not shown here) led to E_{ap} values of 12 ± 4 kJ mol^{-1} similar to those obtained for the formation of SmOCl in the 625–850 °C range which is reasonable if considering that this stage is also occurring at this temperature range. The E_{ap} values found indicate that this stage occurs under external mass transfer control [28,29]. It is confirmed by observing that experimental and theoretical reaction rates are of the same order as displayed in Table 1. The E_{ap} values for α values between 0.6 and 0.9 shown in Fig. 8 are parallel indicating that the mechanism of reaction remains the same. The values are of the order of 75 ± 3 kJ mol^{-1}. These values suggest the presence of chemical-mixed control influenced by external mass transfer. The shift from low to high E_{ap} values as the values of α raise is attributed to the evolution of two different mechanisms of reaction: the formation of SmOCl in the first step and the formation of both $SmCl_3$ and $CeCl_3$ in the second. Although this behavior was observed previously [12], the E_{ap} values for the second step are lower in the case of the present work. It is due to the kinetic effect produced by the presence of a higher amount of C allowable to react [13]. Its combined effect with the formation of both liquid chlorides shifts the chemical-mixed control observed in the case of the carbochlorination of Sm_2O_3 [12] to chemical-mixed influenced by external mass transfer observed in the present work.

3.7. Separation method for this mixture

The separation of these oxides at temperatures lower than 700 °C was discussed in previous works [16,30]. At higher temperatures, the simultaneous formation of $CeCl_3$ and $SmCl_3$ is achieved as discussed in the previous section. Then, the separation method should consist in two steps:

(1) The carbochlorination of the CeO_2–Sm_2O_3 mixture using the minimum amount of C needed according to the stoichiometries of Eqs. (6), (9) and (10) to produce $CeCl_3$ and $SmCl_3$ chlorides.
(2) Since no interaction between the initial oxides and the produced chlorides is observed, the chlorides can be separated using differential volatilization or any other physical method taking advantage of the differences on their vapor pressure [25].

4. Conclusions

In this work, the effect of the temperature on the carbochlorination of a CeO_2–Sm_2O_3 mixture was studied. The starting temperature of the carbochlorination is observed at 400 °C where only Sm_2O_3 is carbochlorinated. Between this temperature and 625 °C, this oxide reacts in one stage forming SmOCl (s). Over 650 °C and up to 950 °C, the formation of $SmCl_3$ occurs as a second step. The stoichiometries and temperature ranges of reaction coincide with those of the individual carbochlorination of this oxide [12]. Over 700 °C, the full carbochlorination of CeO_2 in the mixture is achieved with the same stoichiometry of its individual [13].

The E_{ap} values involved in the formation of SmOCl (s) are 79 ± 3 kJ mol^{-1} between 400 and 625 °C and 12 ± 4 kJ mol^{-1} between 650 and 850 °C, respectively. The same value is obtained at higher temperatures. The formation of SmOCl is achieved under external mass transfer control. The E_{ap} value involved on the formation of $SmCl_3$ and $CeCl_3$ is of the order of 75 ± 3 kJ mol^{-1}. The stage is assumed to be under chemical-mixed control influences by external mass transfer.

Although no interactions between the oxides are observed, a global acceleration of the carbochlorination ratio of the mix-

ture is observed. It is attributed to the presence of a higher amount of carbon available to react per surface area [13] and the formation of liquid $SmCl_3$ which not only enhances the further carbochlorination of SmOCl formed in the first stage but also favors the full carbochlorination of CeO_2 between 700 and 800 °C by coalescing and exposing the unreacted CeO_2 surface to chlorine chemical attack. The simultaneous formation of both liquids at higher temperatures also increases the global reaction rate of the carbochlorination.

As a conclusion, a two-step method based on the carbochlorination and further vaporization of the chlorides to separate the oxides in the initial mixture is proposed.

Appendix A

A.1. Refinements

SmOCl phase was refined with the *P*4/*nmm* space group. Cell parameters *a*, *b* and *c* are equal to 3.982, 3.982 and 6.712 Å, respectively. α, β and γ angles are equal to 90°. Atoms Wyckoff position of SmOCl used during Rietveld refinements were Sm (2c), O (2a) ($z = 0.17$) and Cl (2c) ($z = 0.63$). *z* stands for the adjustable parameter.

Cubic Sm_2O_3 phase was refined with the *Ia*3 space group. Cell parameter *a* is equal to 10.92 Å. α, β and γ angles are equal to 90°. Atoms Wyckoff positions were Sm1 (8b), Sm2 (24d) and O (48e).

Cubic CeO_2 phase was refined with the *Fm*3*m* space group. Cell parameter *a* is equal to 5.398 Å. α, β and γ angles are equal to 90°. Atom Wyckoff positions are Ce (4a) and O (8c).

A.2. Mass balances

As used in previous works [12,13], mass balances were performed in this system to assess the reaction stoichiometries. Two representative temperatures were selected to explain how the mass balances were done: 700 and 950 °C. Both TG curves are displayed in Fig. 9a and b, respectively. In "A" point at Fig. 9a, the initial constituents are: Sm_2O_3 (s), CeO_2 (s) and C (s). At that point, Cl_2 (g) is injected. Between "A" and "B", only Sm_2O_3 reacts according to Eq. (5). CeO_2 presents no reaction at this temperature. At "B" point, $SmCl_3$ (s, l), CeO_2 (s) and C (s) are present. At this point, Cl_2 (g) injection is closed and $SmCl_3$ (l, s) is vaporized in Ar at 950 °C. After that, only CeO_2 (s) and C (s) remain in the crucible. Crucible is weighed and removed. C (s) is burning in air at 950 °C. Remaining CeO_2 (s) is weighed. A resume of results is displayed in Table 3.

In "A" point in Figs. 9b, the initial constituents are the same as the previous case. Between "A" and "B" Sm_2O_3 and CeO_2 react according to Eqs. (10) and (6), respectively. At "B" point, the compounds present are $SmCl_3$ (l, s), $CeCl_3$ (l, s) and remaining C (s). At this point, Cl_2 (g) injection is closed and the chlorides mixture is evaporated in Ar (g) at 950 °C. After that, remaining C (s) is burning in air and the crucible is weighed. A resume of results is also displayed in Table 3. In all cases, chlorine adsorption on C surface and oxidation of C was considered in the mass balances [31].

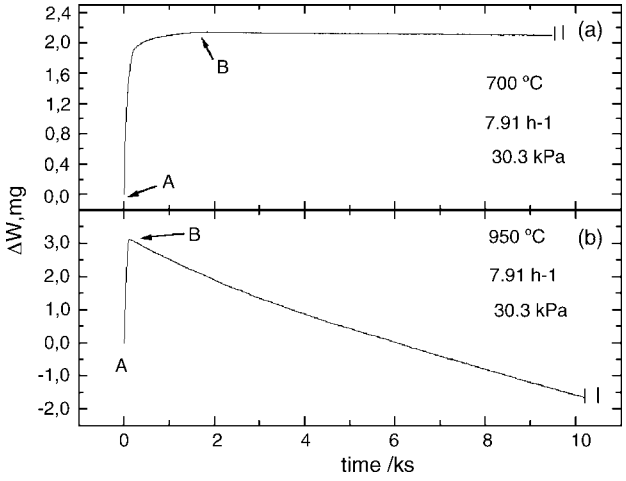

Fig. 9. (a) TG curve at 700 °C and (b) at 950 °C. Both curves are used to exemplify the mass balances performed in this system.

Table 3
Examples of mass balances used to determine the stoichiometries of the reactions involved in this system

T (°C)	Substances	Masses measured in points shown in Fig. 9 (mg)		Masses measured after evaporation in Ar (g)* and burning in Air** (mg)
		A	B	
700	Sm_2O_3	4.468	0	0
	CeO_2	4.468	4.468	4.468
	$CeCl_3$	0	0	0
	$SmCl_3$	0	6.550	0
	C	0.995	0.764	0.764*, 0**
950	Sm_2O_3	4.490	0	0
	CeO_2	4.490	0	0
	$CeCl_3$	0	6.610	0
	$SmCl_3$	0	6.429	0
	C	1.066	0.166	0.166*, 0**

References

[1] Y. Wang, T. Mori, J.G. Li, Y. Yajima, Sci. Technol. Adv. Mater. 4 (2004) 229–238.
[2] J.G. Li, T. Ikegami, T. Mori, Acta Mater. 52 (8) (2004) 2221–2228.
[3] A.M.T. Silva, R.R.N. Marques, R.M. Quinta-Ferreira, Appl. Catal. B 47 (2004) 269–279.
[4] M.P. Kapoor, Y. Ichihashi, T. Nakamori, Y. Matsumura, J. Mol. Catal. A 213 (2004) 251–255.
[5] Q. Zeng, Z. Pei, Q. Su, S. Lu, J. Lumin. 82 (3) (1999) 241–249.
[6] U. Baisch, D. Dell'amico, F. Calderazzo, R. Conti, Inorg. Chim. Acta 357-5 (2004) 1538–1548.
[7] R.G. Haire, L. Eyring, Comparisons of the binary oxides Handbook of the Physics and Chemistry of the Rare Earths, vol. 18, Norh Holland, Amsterdam, 1994 (Chapter 25).
[8] T. Sato, Thermochim. Acta 148 (1989) 249–260.

[9] Y.G. Wang, Y. Xiong, S.L. Meng, D.Q. Li, Talanta 63 (2) (2004) 239–243.
[10] Y.L. Zhang, W.H. Jiang, W.S. Liu, Y.H. Wen, K.B. Yu, Polyhedron 22 (13) (2003) 1695–1699.
[11] C.K. Gupta, C.N. Krishnamurthy, Extractive metallurgy of the rare earths, Int. Mater. Rev. 37 (5) (1992) 217–226.
[12] M.R. Esquivel, A.E. Bohé, D.M. Pasquevich, Thermochim. Acta 403 (2003) 207–218.
[13] M.R. Esquivel, A.E. Bohé, D.M. Pasquevich, Trans. Inst. Min. Metall. (Sect. C: Miner. Process. Extract. Metall.) 111 (2002) C149–C155.
[14] M.R. Esquivel, A.E. Bohé, D.M. Pasquevich, J. Mater. Process. Technol. (in press).
[15] M.R. Esquivel, A.E. Bohé, D.M. Pasquevich, Thermochim. Acta 398 (2003) 81–91.
[16] M.R. Esquivel, A.E. Bohé, D.M. Pasquevich, in: J.P. Barbosa, A.J. Dutra, R. Melamed, R. Trindade (Eds.), Proceedings of the Sixth Southern Hemisphere Meeting on Mineral Technology, vol. 2, 2001, pp. 468–474.
[17] DBWS, 9411 an upgrade of the DBWS programs for Rietveld refinement with PC and mainframe computers, J. Appl. Cryst. 28 (1995) 366–367.
[18] D. Pasquevich, A. Caneiro, Thermochim. Acta 156 (2) (1989) 275–283.
[19] D. Brown, Halides of Lanthanides and Actinides, Wiley, London, 1968.
[20] Joint Committee for Powder Diffraction Standards, Powder Diffraction File, International Center for Diffraction Data, Swarthmore, PA, 1984 (card number 340394).
[21] International Committee for Powder Diffraction Standards, Powder Diffraction File, International Center for Diffraction Data, Swarthmore, PA, 1993 (card number 431029).
[22] Joint Committee for Powder Diffraction Standards, Powder Diffraction File, International Center for Diffraction Data, Swarthmore, PA, 1996 (card number 120790).
[23] Joint Committee for Powder Diffraction Standards, Powder Diffraction File, International Center for Diffraction Data, Swarthmore, PA, 1996 (card number 120789).
[24] Joint Committee for Powder Diffraction Standards, Powder Diffraction File, International Center for Diffraction Data, Swarthmore, PA, 1996 (card number 120791).
[25] S. Boghosian, G.N. Papatheodorou, Handbook of the Physics and Chemistry of the Rare Earths, vol. 23, North-Holland, Amsterdam, 1996 (Chapter 157).
[26] G. Hakvoort, Thermochim. Acta 233 (1994) 63–73.
[27] L.K. Doraiswamy, M.M. Sharma, Heterogeneous Reactions: Analysis, Examples and Reactor Design, vol. 1, Wiley, New York, 1984, p. 149 (Chapter 7).
[28] J. Szekely, J. Evans, H.Y. Sohn, Gas–Solid Reactions, Academic Press, New York, 1976, pp. 109–110 (Chapter 4).
[29] F. Habashi, Principles of Extractive Metallurgy, vol. 1, Gordon and Breach, New York, 1969, pp. 143–144 (Chapter 7).
[30] M.R. Esquivel, A.E. Bohé, D.M. Pasquevich, in: I. Gaballah, B. Mishra, R. Solozabal, M. Tanaka (Eds.), Proceedings of the 2004 Global Symposium on Recycling, Waste Treatment and Clean Technology REWAS'04, vol. 3, 2004, pp. 2275–2284.
[31] J. Gonzalez, M.C. Ruiz, A.E. Bohé, D.M. Pasquevich, Carbon 37 (1999) 1979–1988.